Microstructural Evolution and Mechanical Properties of Braze Joints in Ti-13.4Al-21.2Nb

The process used to manufacture braze foils causes substantial differences in braze joint strength

BY C. H. CADDEN, N. Y. C. YANG AND T. H. HEADLEY

ABSTRACT. Braze joints in Ti-13.4Al-21.2Nb were made using several filler metal compositions based upon the Ti-Cu-Ni ternary system. Specimens were vacuum brazed, using filler metal preplaced between bonding surfaces. Two types of braze foil, one produced by rapid solidification techniques and one formed by a roll bonding process, were examined.

Mechanical test results indicated that substantial differences in braze joint strength could be obtained from specimens prepared using foil manufactured by the two different processes. Specifically, for the higher alloyed composition, a laminated foil produced joints with lower room temperature tensile strength compared to its rapidly solidified counterpart. Specimens prepared using laminated foil typically failed through the braze joint and had low strength. This behavior was related to the presence of an increased amount of centerline alpha-two phase in the braze joints made using the laminated filler metals. The formation of this microstructural feature was influenced by segregation of the filler metal alloying elements, nickel and copper. Braze joints prepared using laminated foils exhibited higher levels of segregation, even after long hold times at the brazing temperature, than joints made using rapidly solidified foil.

Introduction

Recent advances in high-temperature titanium alloys, particularly the titanium aluminide intermetallic alloys, have led to their incorporation in products where their high specific strength can be exploited. To utilize the full capability of these alloys, joining techniques yielding high-integrity bonds are required. In some cases, vacuum brazing is the preferred joining method.

The ordered Ti_3Al intermetallic composition, known as alpha-two, is characterized by good strength, but unacceptably low toughness, particularly at ambient temperatures. Niobium additions have been found to dramatically improve the balance of mechanical properties, although room temperature ductility remains limited (Ref. 1). Ti-14Al-21Nb (wt-%) is a first generation alpha-two composition that has been the basis of numerous detailed studies. While not considered a viable candidate for commercial applications, this alloy has provided a baseline for understanding the thermal and mechanical response of alpha-two titanium aluminides.

Previous investigations (Ref. 2) have indicated that filler metals based on the Ti-Cu-Ni system can produce alpha-two titanium aluminide braze joints with good mechanical integrity. Due to the presence of brittle intermetallic compounds in the Ti-Cu-Ni alloy system, filler metals are not produced by conventional ingot metallurgy processes. Laminated foils are fabricated by roll bonding titanium sheets on both sides of a copper-nickel core. Alternatively, rapid solidification technology (meltspinning) is employed to manufacture foil in the form of cast ribbons. The meltspun product is amorphous (or nearly so) with a high degree of chemical homogeneity (Ref. 3), while the laminated foils are very inhomogeneous, having all of the solute elements in the center between layers of pure titanium. It has previously been noted (Ref. 2) that substantial differences in mechanical properties can be obtained from joints fabricated using laminated vs. meltspun filler metal of the same composition. Reportedly, homogeneous amorphous filler metal foils produce superior braze joints in a number of alloy systems (Refs. 3–5), although reasons for this behavior are unclear.

Detailed analyses were performed in the present study to characterize microstructures formed in Ti-13.4Al-21.2Nb braze joints prepared using filler metals from the Ti-Cu-Ni alloy system.

KEY WORDS

Braze joints
Ti-13.4Al-21.2Nb
Alpha-two composition
Ti-Cu-Ni ternary system
Laminated foil
Meltspun foil

Experimental Section

Ti-13.4Al-21.2Nb (wt-%) plate having a thickness of 2.5 cm (1 in.) was vacuum heat treated for 30 min at a temperature of 1150°C (2102°F), well above the reported beta transus temperature of 1000°C (1832°F) (Ref. 6). A gas fan cool from the hold temperature produced a creep-resistant microstructure (Ref. 4) consisting of coarse, equiaxed prior beta grains of 2 to 3 mm (0.08 to 0.12 in.) diameter and plates of Widmanstätten alpha-two (light phase) separated by thin ribs of untransformed beta (dark phase), as shown in Fig. 1. The heat-treated plates were then cut into 2.5-cm cubes for brazing experiments. One face of each cube was ground using 240-grit abrasive.

Five commercially available Ti-Cu-Ni filler alloys were evaluated. Laminated

C. H. CADDEN and N. Y. C. YANG are with Sandia National Laboratories, Livermore, Calif. T. H. HEADLEY is with Sandia National Laboratories, Albuquerque, N. Mex.

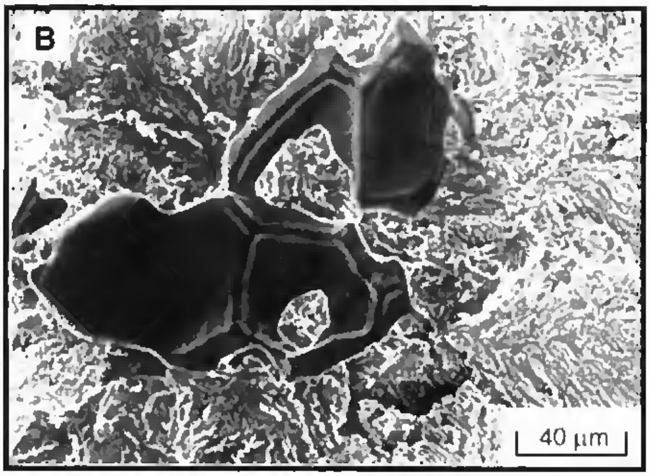

Fig. 1 — Ti-13.4Al-21.2Nb plate microstructure following beta heat treatment: Widmanstätten alpha-two plates (light phase) separated by untransformed beta.

Table 1 — Melting Characteristics of Ti-Cu-Ni Filler Metals

Braze Alloy	Thickness μm (in.)	Solidus* °C (°F)	Liquidus* °C (°F)
Ti-15Cu-15Ni			
Meltspun	40 (0.0016)	902 (1656)	932 (1710)
Laminated	39 (0.0015)	912 (1674)	1007 (1845)
Ti-20Cu-20Ni			
Meltspun	38 (0.0015)	915 (1679)	936 (1717)
Ti-15Cu-25Ni			
Meltspun	38 (0.0015)	901 (1654)	914 (1677)
Laminated	46 (0.0018)	912 (1674)	1007 (1845)

*From Ref. 3.

TiCuNi® foils were procured from WESGO, Inc.; rapidly solidified Metglas® ribbons were supplied by Allied-Signal, Inc. The laminated foils were produced in 101-mm (4-in.) widths while the meltspun foils were supplied in either 3.2- or 12.7-mm (0.125- or 0.5-in.) widths. Composition and foil thickness for each filler material are listed in Table 1. Attempts to determine solidus and liquidus temperatures for each braze alloy, using differential thermal analysis (DTA), produced data that were considered unreliable due to chemical interactions between the molten filler metal and the sample crucible. Published melting characteristics (Ref. 3) of the filler alloys are reported in Table 1.

Prior to assembly of specimens for brazing, all materials were cleaned in acetone, rinsed in methanol and forced hot air dried. Laminated foil was cut into a 3-cm (1.2-in.) square, centered on a polished face of a titanium alloy cube, and resistance spot welded in place at one corner of the face. Because the meltpsun filler metals were not sufficiently wide to allow the use of a single piece, 30.5-mm (1.2-in.) lengths were cut and placed on a cube face to ensure a uniform, single-layer coverage of the surface. The individual foil lengths were then resistance spot welded to the titanium. A brazing specimen was constructed by stacking another titanium cube on top of the first so that the polished sides were facing each other, separated by the layer of desired braze filler metal. Note that for both the laminated and meltspun foils, the spot welds were kept near the perimeter of the specimen and a slight amount [2.5 mm (0.1 in.)] of foil extended past the "joint" edge to ensure sufficient braze coverage. The assembly was then loaded into an electrically heated vacuum furnace; a 22-kg (48.5-lb) tungsten block was placed on top to provide bonding pressure.

The all-metal vacuum furnace was pumped down to a pressure of at least 10^{-5} torr (0.01 psi). Specimens were then heated at a rate of 5°C/min (9°F/ min) to a peak temperature of 982°C (1800°F). A brazing time of 60 min at 982°C was chosen to allow for dissolution of the base metal with a goal of obtaining a strong, ductile joint. (Without substantial dilution of the molten filler metal by base metal elements, a solidified braze joint would contain the brittle phases that prevent manufacturing of these filler alloys by traditional casting and rolling processes.) After holding at temperature for 1 h, power to the heating elements was interrupted and the specimens were allowed to cool in vacuum to ambient temperature. A thermocouple placed inside one assembly indicated that the cooling rate was approximately 40°C/ min (72°F/min) from 982°C to 800°C (1472°F). Typical vacuum leak-up rates were found to be on the order of 8×10^{-6} cm^3(STP)/s (5×10^{-7} $in.^3$/s).

Cylindrical transverse tensile test bars, 50 mm (2 in.) in length, were machined from the brazed specimens with threaded grips and reduced gauge sections measuring 17 mm (0.67 in.) in length by 4 mm (0.16 in.) in diameter. Duplicate tensile tests were conducted at room temperature, 649°C (1200°F) and 760°C (1400°F) using a servohydraulic machine with a crosshead speed of 0.127 mm/min (0.005 in./min). Figure 2 shows a bond specimen in the as-brazed condition and a machined mechanical test bar.

Cross sections of brazed specimens were metallographically mounted and polished. Microstructures and compositions were analyzed using optical microscopy and a JEOL 733 electron microprobe equipped with energy dispersive X-ray spectroscopy (EDS). For selected braze joints, thin foils were prepared by ion milling for observation in a Philips CM30 transmission electron microscope (TEM) also equipped with EDS.

Results and Discussion

All brazing trials produced joints whose microstructures were similar to those shown in Fig. 3. Within the joints there appeared to be nearly equal amounts of light and dark lamellar phases. Epitaxial growth was occasionally evident at the base metal interface, but other areas exhibited no obvious orientation dependence. The joints were characterized by large grains [upwards of 150–200 μm (0.006–0.008 in.) in width]. At some locations, these lamellae spanned the entire joint; in others, the grains met near the braze centerline, creating a continuous phase oriented more or less parallel to the braze joint. Braze joint widths were found to be between 80 and 100 μm (0.003 and 0.004 in.) for all of the nominally 40 μm (0.0016 in.) thick filler metals, indicating that the molten filler metal had indeed been substantially diluted. Note that despite a brazing temperature 25°C (77°F) below the reported liquidus temperature of the laminated filler metals (982 vs. 1007°C), there was no evidence of incomplete melting of these foils.

Results of tensile testing are shown in Table 2. At elevated temperatures, all failures were associated with the braze joint and strengths were considerably below the values listed for the parent material. At room temperature, the lower alloyed filler metals produced joints possessing

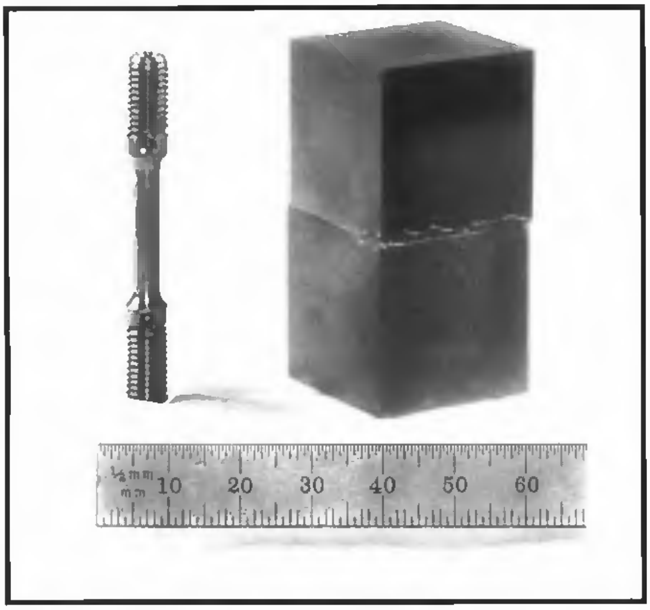

Fig. 2 — Bond specimen in the as-brazed condition and a machined mechanical test bar.

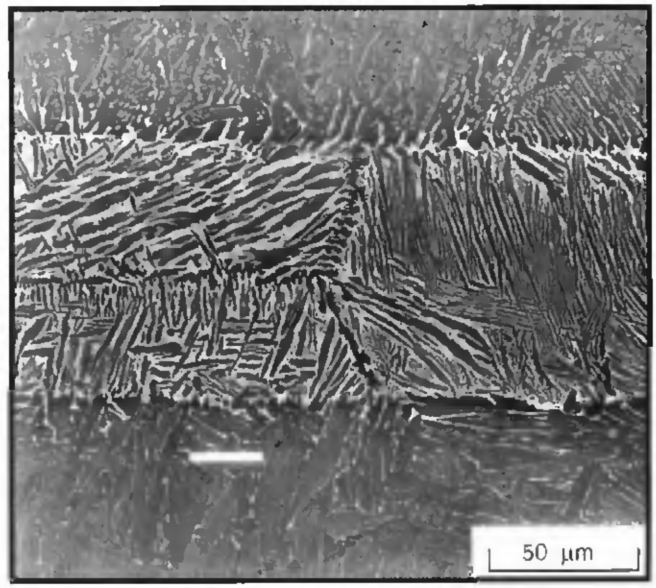

Fig. 3 — Microstructure of specimen brazed using meltspun Ti-15Cu-15Ni. Rectangular area represents orientation and size of microprobe sample area for compositional analyses.

parent material strengths, with failures located outside of the braze region. However, the more highly alloyed Ti-15Cu-25Ni composition produced mixed results. Specimens made using the meltspun foil produced base metal failures, while the laminated Ti-15Cu-25Ni produced joints with poor room temperature strength, characterized by braze joint failures.

Several room temperature fracture surfaces from the laminated Ti-15Cu-25Ni joint were mounted in an epoxy. A plane was ground and polished perpendicular to each fracture surface to reveal the precise location of failure in the braze joint. After dissolution of the epoxy material, examination of the specimens (Fig. 4) revealed a predominantly transgranular fracture, through plates, with distinct areas of intergranular failure. Fracture surfaces were completely contained within the braze joint. The intergranular surfaces appeared to be associated with the continuous centerline phase. The amount of this centerline structure was quantified by examining at least 25 mm (1 in.) of braze joint microstructure for each of the filler metals. The segments of centerline phase were then totaled and compared to the total joint length examined. Table 3 lists the quantities of centerline phase associated with each filler metal. The laminated Ti-15Cu25-Ni joint length contained almost 50% of this feature; all other joints exhibited lesser amounts.

The electron microprobe was used to characterize solute segregation within the braze joint. This was accomplished by measuring the composition of a 3 x 25 μm (0.00012 x 0.001 in.) area and indexing the location of that area in 1-μm (0.00004-in.) increments across the braze joint. The 25-μm dimension was oriented parallel to the braze joint, effectively in-

Table 2 — Tensile Properties[a] for Ti-13.4Al-21.2Nb Joints Brazed at 982°C (1800°F) for 1 h with Various Ti-Cu-Ni Filler Metals

	22°C (72°F)				649°C (1200°F)				760°C (1400°F)			
Filler Metal	0.2% Yield Strength	Ultimate Tensile Strength	% R.A.	Failure Location	0.2% Yield Strength	Ultimate Tensile Strength	% R.A.	Failure Location	0.2% Yield Strength	Ultimate Tensile Strength	% R.A.	Failure Location
Ti-15Cu-15Ni												
Meltspun	465 (67)	516 (75)	1	Base Metal	253 (37)	464 (67)	17	Bond	248 (36)	312 (45)	5	Bond
Laminated	433 (63)	518 (75)	1	Base Metal	253 (37)	429 (62)	12	Bond	221 (32)	281 (41)	2	Bond
Ti-20Cu-20Ni												
Meltspun	481 (70)	547 (79)	2	Base Metal	243 (35)	485 (70)	22	Bond	221 (32)	344 (50)	6	Bond
Ti-15Cu-25Ni												
Meltspun	482 (70)	548 (80)	2	Base Metal	243 (35)	485 (70)	22	Bond	221 (32)	344 (50)	6	Bond
Laminated	—	400 (58)	1	Bond	256 (37)	480 (69)	15	Bond	240 (35)	302 (44)	5	Bond
Ti-15Cu-15Ni + Ni Coat												
Laminated	471 (68)	523 (76)	1	Base Metal	255 (37)	472 (68)	18	Bond	237 (34)	317 (46)	5	Bond
Base Metal[b]	455 (66)	526 (76)		—	305 (44)	540 (78)		—	278 (40)	472 (68)		—

(a) Values reported in MPa and ksi.
(b) Material previously exposed to 982°C/1 h brazing thermal cycle.

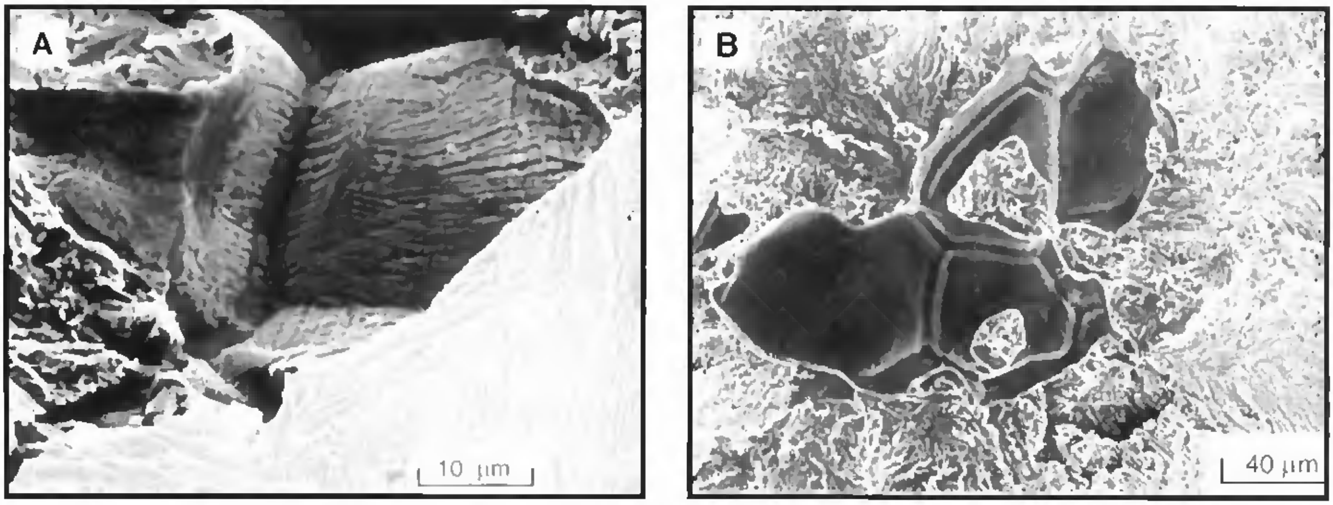

Fig. 4 — Fracture surface from room temperature test of specimen brazed using laminated Ti-15Cu-25Ni. A — Fracture surface contained within braze microstructure. B — Failure exhibits both intergranular and transgranular components.

cluding several of the light and dark lamellae as shown in Fig. 3. A plot of composition vs. location for the laminated Ti-15Cu-15Ni is shown in Fig. 5. (Titanium content was an almost constant 65 wt-% in the base metal and throughout the braze joint for all specimens; consequently it is not displayed on the microprobe traces reported here.) Near the joint boundary, there is a steep composition gradient of both copper and nickel, indicative of only limited diffusion of these solute atoms in the base metal. Within the joint itself, there is a nearly constant concentration of nickel, copper and aluminum, while niobium shows more of a compositional gradient. Joints made using both the laminated Ti-15Cu-15Ni and the meltspun Ti-20Cu-20Ni filler metals exhibited similar compositional profiles.

The Ti-15Cu-25Ni filler metals produced joints (Figs. 6 and 7) having less compositional uniformity. In particular, the nickel content varied locally across the width of the joints. This effect was more pronounced in joints made with laminated foil where local concentrations of 13 or 14 wt-% nickel were measured. (Note that in Fig. 7, a series of nickel "peaks" appears to be symmetric about the center of the joint, suggesting that this segregation phenomenon might be controlled by diffusion-limited processes.) Because the light and dark lamellae are likely to have different chemistries, the local composition measured by microprobe analysis was believed to be sensitive to the percentage of each constituent in the analysis. Consequently, several additional traces were performed for each specimen. Considerable variability was observed regarding the number and location (relative to bond width) of the nickel "spikes" shown in Figs. 5–7. However, the trends were consistent, with the laminated Ti-15Cu-25Ni filler joints invariably exhibiting greater scatter in local nickel content.

Table 3 — Fraction of Braze Joint with Continuous Centerline Phase

Filler Metal	% Continuous Centerline Structure	R.T. Tensile Failure Location
Ti-15Cu-15Ni		
Meltspun	29	Base Metal
Laminated	24	Base Metal
Ti-20Cu-20Ni		
Meltspun	15	Base Metal
Ti-15Cu-25Ni		
Meltspun	30	Base Metal
Laminated	47	Bond
Ti-15Cu-15Ni + Ni Coat		
Laminated	39	Base Metal

An average of all of the data points taken between the braze joint boundaries provides a bulk composition of the melt zone for each joint. These data, shown in Table 4, indicate that the joint compositions were very similar for all of the filler metal compositions. Note that the average nickel content was nearly constant despite a considerable difference (15, 20, 25%) in original filler metal nickel content. However, increasing filler metal nickel content resulted in joints with decreased amounts of copper and increased niobium content. Despite the dissimilarity in tensile properties, meltspun and laminated Ti-15Cu-25Ni foils produced joints with very similar bulk compositions. The observed disparity in mechanical properties is evidently the result of localized chemical or structural differences.

A pseudobinary equilibrium phase diagram proposed by Bendersky, *et al.* (Ref. 8), for the Ti_3Al- Nb system is shown in Fig. 8. According to the diagram, the low-temperature equilibrium microstructure of the base metal composition (10.9 at. % niobium) should consist of both DO_{19}, an ordered hexagonal close packed (HCP) phase, and an orthorhombic phase (O). However, TEM analysis of the base metal indicated that it consisted of primarily DO_{19} with small amounts of untransformed body-centered cubic (BCC) phase (dark boundaries separating plates in Fig. 1). The importance of cooling rate on weld fusion zone microstructures in this alloy has been well documented by several investigators (Refs. 9–12). In the current study, the cooling rate from the initial heat treatment was measured at approximately 200°C/ min (360°F/min), considerably slower than the rates found in most fusion welds, but apparently still

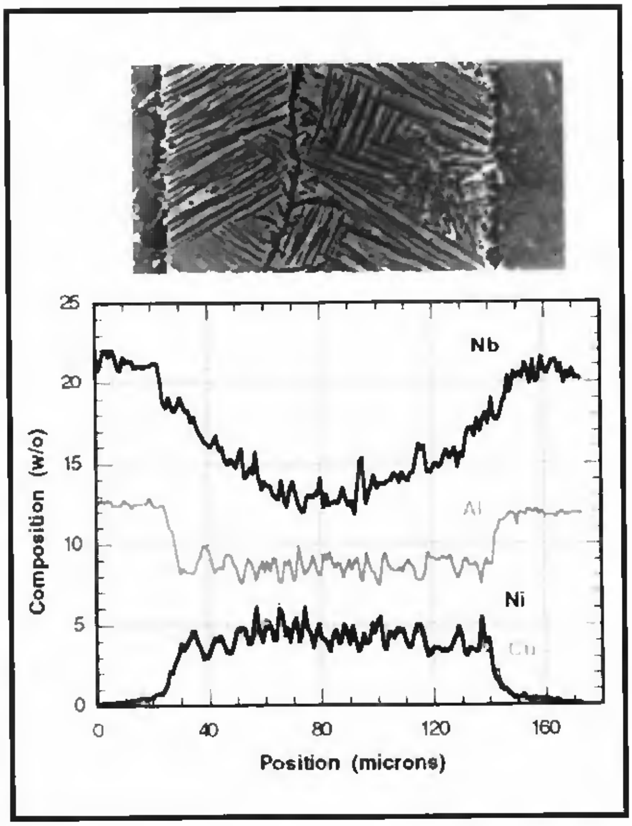

Fig. 5 — Compositional profile across laminated Ti-15Cu-15Ni joint.

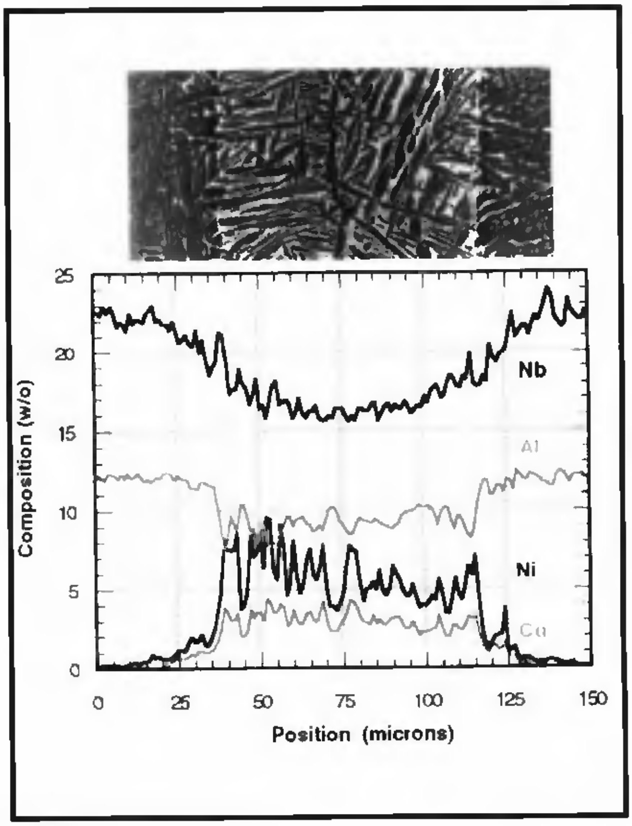

Fig. 6 — Compositional profile across meltspun Ti-15Cu-25Ni joint.

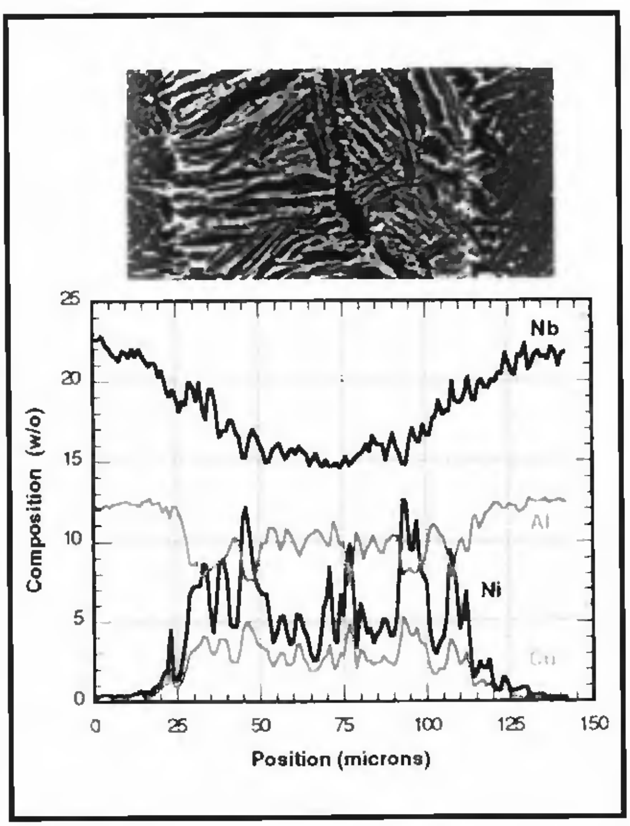

Fig. 7 — Compositional profile across laminated Ti-15Cu-25Ni joint.

fast enough to prevent complete transformation of the high-temperature phase. Even after the comparatively slow 40°C/min cooling rate associated with the braze cycle, the base metal microstructure showed a mixture of DO_{19} (also known as alpha-two) and the beta (BCC) phases, rather than the DO_{19} and orthorhombic phase structure found hy 8endersky (Ref. 8).

A TEM image of a typical braze microstructure from the meltspun Ti-15Cu-25Ni foil is shown in Fig. 9. Three prominent phases were found in joints prepared using both forms of this filler metal composition, rather than simply two lamellar phases as suggested in Fig. 3. Selected area diffraction (SAD) permitted identification of the three phases; a fourth, which only comprised an estimated 3% of the overall volume, has not yet been identified. Table 5 lists the approximate relative amounts of these phases, estimated from TEM images, and their respective compositions. The results indicate that the dark contrast phase seen in Fig. 3 is the DO_{19} phase, which is separated by ribbons of both BCC and other intermetallic phases. The two intermetallic phases, identified as I_1 and I_2, were found to contain most of the copper and nickel. The I_1 phase was found to have an orthorhombic structure, although the lattice constants (a_o = 0.972 nm, b_o = 1.004 nm, c_o = 0.829 nm) indicate that it is not the same orthorhombic Ti_2AlNb compound (O) referred to in Fig. 8 (Ref. 13). These metastable phases are known to have inferior creep strength compared to predominantly alpha structures (Ref. 14). The poor high- temperature tensile properties of the brazed specimens can be attributed to the increased proportion of beta and orthorhombic phases present in the joint area.

Microstructural Evolution

In titanium alloys, aluminum tends to stabilize the alpha (HCP) phase while niobium enhances beta (BCC) phase stability (Ref. 15). Nickel and copper are also beta stabilizers, although not as potent as niobium (in binary alloys). While the melt zone compositions (Table 4) show a decrease in niobium content in the braze joint compared to the base metal, substantial amounts of both copper and nickel are present. In fact, the sum of the beta stabilizers (copper, nickel and niobium) is nearly a constant 24 wt-% (15 at.%) in joints prepared using the five different filler metals. The combination of lower amounts of aluminum (9 wt%, 16 at.%) with the presence of both copper and nickel in the braze joints undoubtedly renders Fig. 8 inexact for these compositions, but it retains some utility for describing microstructural events that occur during cooling. An increase in niobium (or beta stabilizer) content from 10.9 toward 15 at.% will tend to change the balance of microstructural phases present at low temperatures by increasing the amounts of both beta (either BCC or the ordered B2) and O phases present during cooling. Additionally, the temperature stability of the orthorhombic phase increases with beta stabilizer content, thereby improving the probability of a BCC to O transformation during cooling from the brazing temperature.

Microprobe analysis of selected braze joint features was used to characterize their microstructural evolution. Figure 10 shows the composition at several locations near the boundary between base metal and the solidified joint. Solidification at the base metal interface (indicated by arrows) is seen to have occurred epitaxially as a two-phase alpha and beta front proceeding toward the center of the joint. However, this mixture of phases does not reflect the high beta stabilizer content of the solidifying liquid. Consequently, excess copper, nickel and niobium were rejected into the liquid ahead of the advancing solidification front. These increasing concentrations of beta stabilizers in the liquid caused an abrupt change in the solidification mode from alpha to beta. This transition area is evident as a nearly continuous strand of beta/orthorhombic phase oriented parallel to, and within a few micrometers of, the base metal interface. (Note that the composition of Point 5 in Fig. 10 corresponds to that of a mixture of both BCC and O phases, consistent with the morphology observed using TEM.) The short distance between the base metal interface and the transition to beta solidification indicates that diffusion of beta stabilizers in the liquid, away from the solid-liquid interface, is limited. Figures 6 and 7 suggest that nickel, with its particularly pronounced concentration variation (at least in the joints made with higher alloyed filler metals), diffuses the slowest. The wide range of allowable beta compositions (Fig. 8) suggests that the excess beta stabilizer can be accommodated in the beta solidification. Thereafter, solidification proceeds as a leaner beta composition consistent with the bulk liquid chemistry. While cooling to room temperature, the large beta grains in the braze joint undergo solid state transformations to produce the mix of phases previously described, while the enriched transition area is less likely to transform to the DO_{19} structure.

The continuous centerline phase (Fig. 11) was found to have the DO_{19} (alpha-two) composition, while areas immediately adjacent (light contrast) appeared to consist of predominantly the I_1 orthorhombic composition. It is quite common to find alpha phase decoration at prior beta grain boundaries in commercial $\alpha + \beta$ titanium alloys that have been quenched from above the beta transus. Because beta stabilizers in these alloys (generally vanadium and molybdenum) partition strongly to the beta phase, the beta grain boundaries consist of the most dilute beta obtainable, which readily exhibit nucleation and growth of alpha phase on cooling (Ref. 16). How-

Table 4 — Melt Zone Chemistries (w/o) for Ti-14Al-21Nb Braze Joints

Filler Metal	Ti	Cu	Ni	Nb	Al	Cu + Ni + Nb
Ti-15Cu-15Ni						
Meltspun	66.7	4.4	4.5	15.4	9.0	24.4
Laminated	68.8	3.9	3.9	14.8	8.7	22.6
Ti-20Cu-20Ni						
Meltspun	66.7	3.8	4.3	16.0	9.3	24.1
Ti-15Cu-25Ni						
Meltspun	65.6	2.5	4.8	17.5	9.7	24.8
Laminated	65.5	2.5	5.1	17.1	9.9	24.7
Ti-15Cu-15Ni + Ni Coat						
Laminated	65.7	3.0	4.8	16.8	9.6	24.6

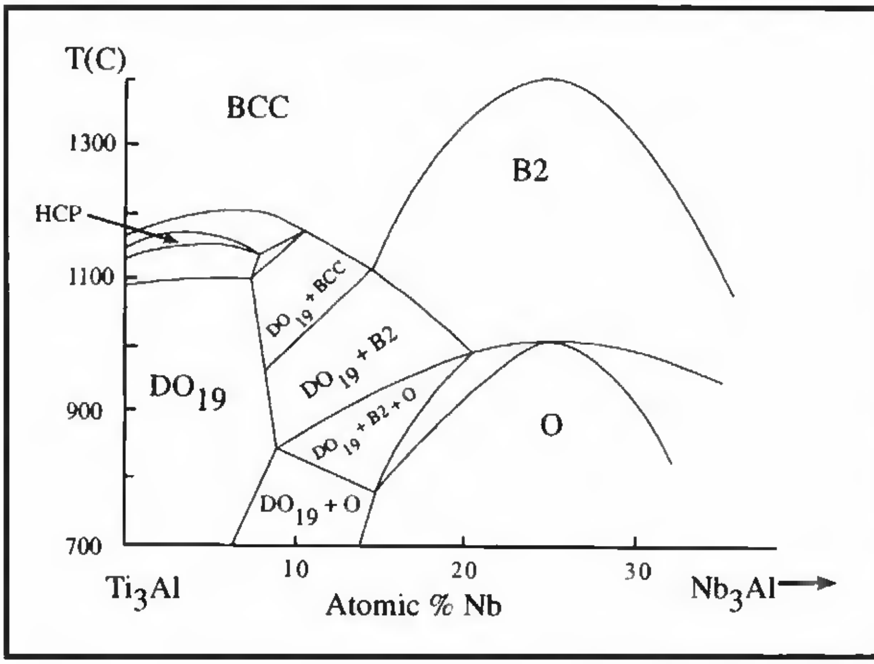

Fig. 8 — Pseudobinary equilibrium phase diagram for Ti_3Al-Nb (Ref. 8).

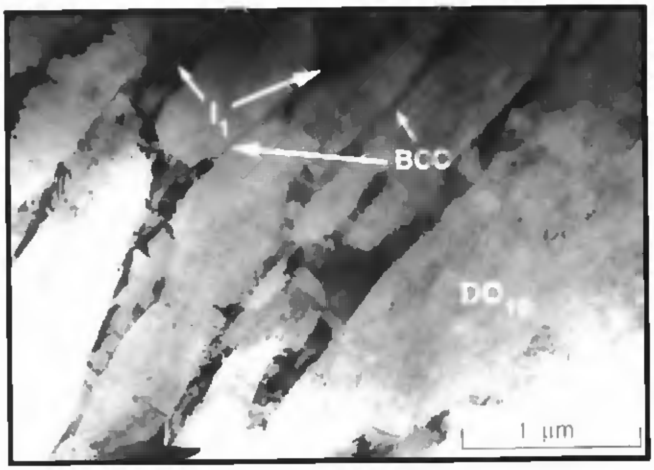

Fig. 9 — TEM bright-field micrograph of joint microstructure from meltspun Ti-15Cu-25Ni specimen.

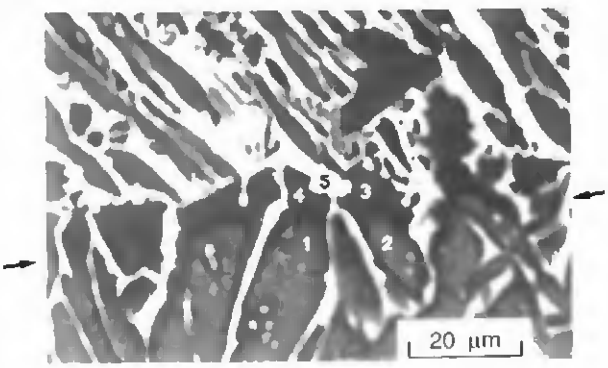

	Ti	Cu	Ni	Nb	Al
Point 1	68.0	0.5	0.4	21.5	12.6
2	67.4	0.4	0.3	21.7	13.0
3	70.5	0.6	0.3	17.9	12.9
4	69.7	0.5	0.4	17.3	13.2
5	62.0	3.7	4.0	21.7	13.0

Fig. 10 — Microstructure and EDS analysis of boundary (arrows) between base metal and solidified joint for laminated Ti-15Cu-25Ni specimen.

ever, the presence of the nickel-, copper- and niobium-rich orthorhombic phase in close proximity to the grain boundary alpha-two phase suggests that evolution of the microstructure in these braze joints follows a different path. Electron microprobe scans across the braze joints, particularly those from the Ti-15Cu-25Ni filler metals (Figs. 6, 7), show areas of high nickel concentration near the center of the joint. This effect could be the result of initial segregation in the braze joint (from incomplete homogenization of the molten filler metal) or it could be caused by solute partitioning during solidification.

To investigate the transport of nickel and copper through the braze joint, specimens were prepared using both the meltspun and laminated Ti-15Cu-25Ni foils, according to the procedures detailed previously. However, the thermal cycle was changed to limit the high-temperature exposure to a total of 2 min compared to the baseline of 1 h. Metallographic results (Figs. 12 and 13) indicated that the resulting joints were much narrower (~50 vs. ~80 μm) than the baseline joints (1 h at 982°C), again indicative of the slow diffusion of solute elements and subsequent dissolution of base metal. Both of the 2-min joints contained considerable segregation towardsthe center. Large but discrete particles were seen in the joint prepared with meltspun foil, while the laminated foil produced a joint that contained a continuous region of two phases in the center. Chemical analysis indicated that the same nickel-rich phase was present in both joints. Additionally, the laminated joint contained an intermittent phase (Point 1 in Fig. 13) consisting of substantial amounts of both copper and nickel. It is clear from the figures that the meltspun filler metal produced a more homogeneous joint during the 2-min hold time at 982°C. Because both joints were formed using filler metal of the same bulk composition and experienced the same thermal history, the more pronounced segregation found in the laminated joint seems likely to be a result of the initial copper and nickel distribution in the center of the filler metal foil compared to the more uniform composition of the meltspun foil.

This characteristic slow diffusion of solute species through the liquid influences microstructural development in the entire joint in two respects. The limited transport of solute (particularly nickel) away from the initial solidification front has been previously described. However, the development of microstructure in the center of the joint is affected in large part by the incomplete homogenization of the liquid phase at the brazing temperature of 982°C. As filler metal nickel content increases, the differences in solute distribution in the laminated vs. meltspun joints is magnified, resulting in the noticeably different terminal solidification microstructures shown in Figs. 12 and 13.

The following solidification sequence near the bond centerline is proposed. With the approach of beta grains from opposing sides of the joint, the effect of nickel and copper rejection into the liquid ahead of the solidification front, combined with the high residual nickel in the center of the joint, can cause beta solidification to become unstable (as shown in Figs. 12 and 13). In areas of particularly high solute content, solidification changes to an orthorhombic structure (or B2, which subsequently transforms to O phase) to accommodate the increased nickel and copper levels. This ortho-

Table 5 — Composition (w/o) of Phases in Base Metal and Braze Joints Made with Ti-15Cu-25Ni Filler Metals

		Ti	Al	Nb	Ni	Cu
DO_{19}	Meltspun	68.4	14.5	15.2	0.2	1.7
(0.50)	Laminated	69.8	14.2	14.3	0.3	1.4
BCC	Meltspun	61.5	3.1	31.7	2.0	1.7
(0.17)	Laminated	62.7	3.7	29.1	1.9	2.6
I_1	Meltspun	48.3	5.1	10.8	22.0	13.9
(0.30)	Laminated	48.3	5.3	11.6	25.5	9.3
I_2	Meltspun	54.5	1.2	4.8	16.6	23.4
(0.03)	Laminated	55.0	1.1	4.4	16.7	22.4
DO_{19}	Base Metal	64.8	14.4	19.5	—	—
BCC	Base Metal	53.1	3.9	41.8	—	—

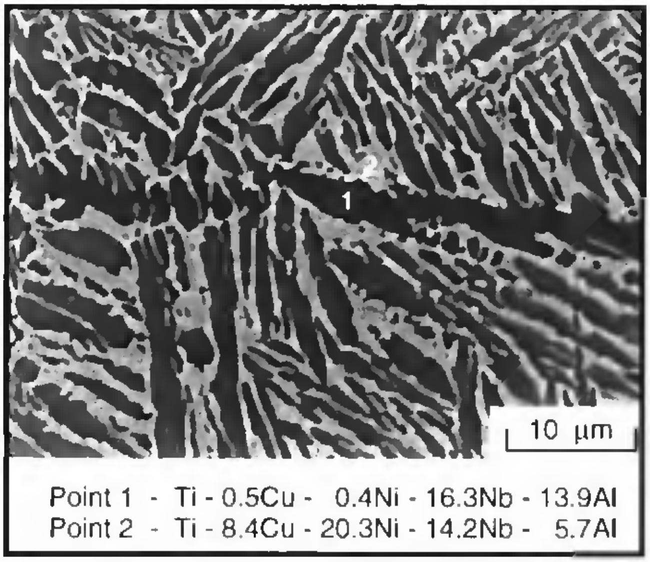

Fig. 11 — Microstructure and EDS analysis of joint centerline features in meltspun Ti-15Cu-25Ni specimen.

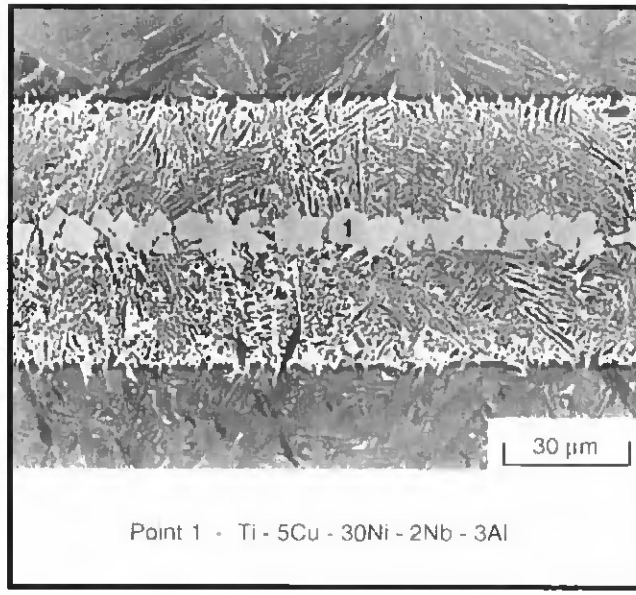

Fig. 12 — Microstructure and EDS analysis of meltspun Ti-15Cu-25Ni specimen brazed at 982°C (1800°F) for 2 min.

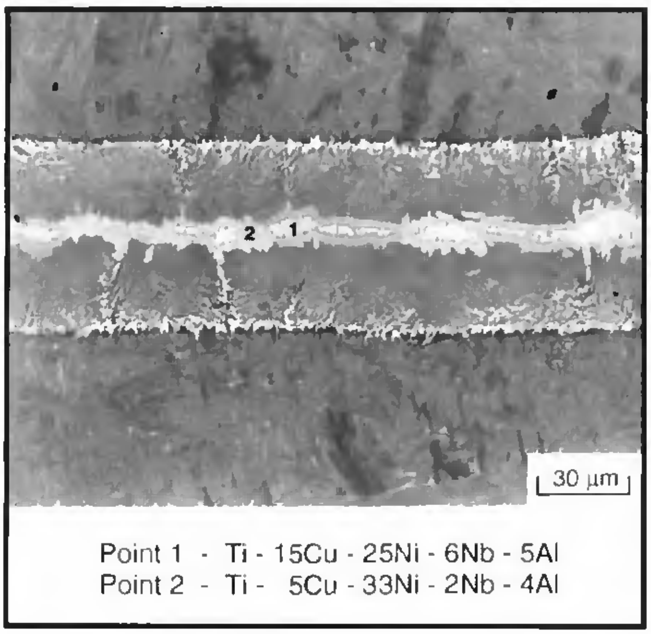

Fig. 13 — Microstructure and EDS analysis of laminated Ti-15Cu-25Ni specimen brazed at 982°C (1800°F) for 2 min.

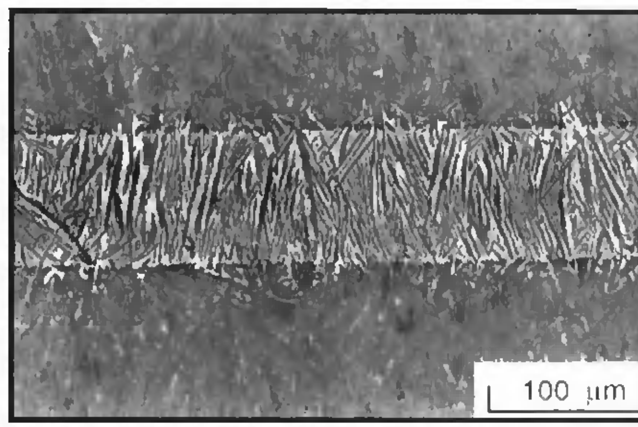

Fig. 14 — Selected area of Ti-20Cu-20Ni joint showing lack of centerline features.

rhombic (or B2) solidification, oriented parallel to the solidification front, then consumes the remaining solute content. The very last region to solidify, at the boundary between the two solidification fronts, would be less rich in beta stabilizers. This narrow band of nickel-, copper- and niobium-depleted solid (compared to the bulk intermetallic composition) acts as a nucleation site for transformation to the close-packed DO_{19} phase upon further cooling. Liquid regions, which have a lower solute content as the beta grains converge near the centerline, do not undergo the transformation to orthorhombic (or B2) solidification. At these locations, a boundary is formed where beta grains meet. Subsequent solid-state transformations (beta to DO_{19} and beta to orthorhombic) remove any distinctive microstructural discontinuity; a smooth transition between orientations is evident in Fig. 14.

To test the sensitivity of microstructure to nickel distribution, a second type of laminated Ti-15Cu-25Ni foil was fabricated. A thin nickel layer was sputter deposited on both sides of a piece of laminated Ti-15Cu-15Ni foil. To obtain the desired bulk composition, it was first necessary to remove some of the pure titanium layer. After weighing a 100 mm x 100 mm x 37 μm (4 x 4 x 0.002 in.) square of Ti-15Cu-15Ni, 7.3% of the weight of the foil (only titanium) was removed by chemically etching in a dilute solution of HNO_3 and HF. Subsequent controlled deposition of nickel on both sides of the foil produced a bulk composition of Ti-14.5Cu-24.9Ni. A specimen brazed at 982°C for 1 h produced the joint microstructure shown in Fig. 15.

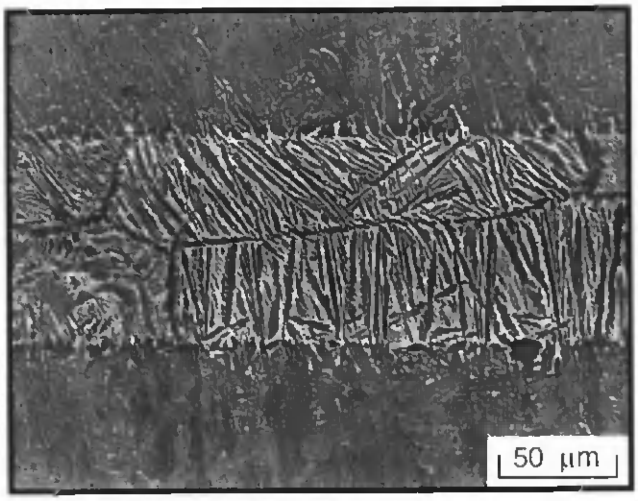

Fig. 15 — Microstructure of joint prepared using "custom" Ti-15Cu-25Ni layered foil.

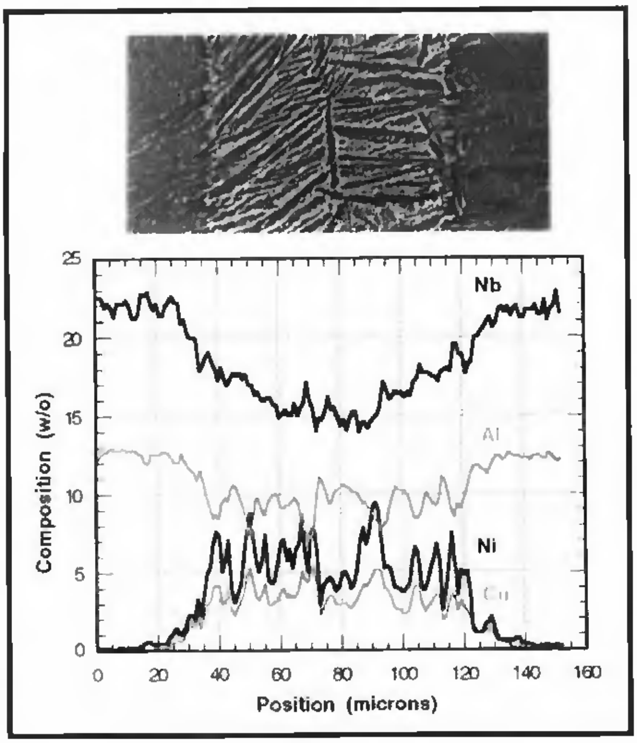

Fig. 16 — Compositional profile across joint prepared using "custom" Ti-15Cu-25Ni.

This joint contained 39% of centerline DO_{19} phase, a value midway between those measured for meltspun and commercially prepared laminated foils. The nickel concentration appears to be more uniform than that found in the "standard" laminated Ti-15Cu-25Ni foil; microprobe results (Fig. 16) also document a reduced nickel concentration toward the center of the joint made with the custom prepared foil (5% vs. 4–10%). The overall braze joint composition (Table 4) was found to be slightly enriched in copper with a corresponding slight reduction in niobium compared to joints prepared with the commercial filler metals of this composition, but well within the range found for the Ti-Cu-Ni alloys. Finally, room temperature tensile specimens prepared using the custom foil broke in the base metal at strength levels comparable to those obtained with the meltspun foil (Table 2). The elevated temperature tensile behavior was also comparable to earlier results.

Conclusions

The brazing studies conducted on Ti-13.4Al-21.2Nb in the current investigation have led to an understanding of some of the factors that determine microstructures and mechanical behavior of brazed components. The following conclusions are drawn from the results of this work:

1) The use of filler metals based upon the Ti-Cu-Ni alloy system can produce braze joints with room temperature tensile strength comparable to alpha-two titanium aluminide parent material. However, at test temperatures of 649°C and 760°C, joints produced with these filler metals have only 70–80% of base metal tensile strength.

2) After a brazing cycle of 1 h at 982°C, laminated and meltspun foils of the same alloy were found to produce joints with nearly identical joint compositions, although the distribution of elements within the joints differed. Meltspun foils, particularly at higher solute compositions, produced joints having a more uniform solute distribution than their laminated counterparts.

3) Braze joint microstructure was shown to be controlled in large part by diffusion of solute elements, particularly nickel. It is proposed that residual solute content in the center of the braze joint determines the microstructure of the final regions to solidify. At those locations where the nickel content was particularly high, the solidification mode can change from beta to an orthorhombic structure, resulting in a final centerline structure that readily transforms to an HCP phase after cooling.

4) Laminated and meltspun Ti-15Cu-15Ni foils produced joints with similar microstructures and chemical compositions using a brazing cycle of 982°C for 1 h.

5) Commercial laminated foil of composition Ti-15Cu-25Ni produced joints with particularly high nickel segregation. High levels of nickel near the center of the joint, a remnant of the initial solute distribution in the filler metal, is believed to have caused an unusually high amount of centerline alpha-two phase that contributed to poor room temperature tensile behavior. By changing the distribution of nickel in a laminated foil, the quantity of centerline alpha-two phase can be reduced, thereby improving room temperature strength. Meltspun foil of this composition exhibited less segregation and produced joints with good room temperature tensile properties. Considering the different microstructural features observed in the 2-min and 60-min braze joints (and probable differences in strength), brazing time and filler metal compositional distribution appear to be critical parameters.

Acknowledgments

This work was performed at Sandia National Laboratories, supported by the U.S. Department of Energy under Contract DE-AC04-94AL85000. The authors are grateful for the consistent craftsmanship of A. Gardea and C. Rood, both of whom contributed to the developments reported here.

References

1. Blackburn, M. J., and Smith, M. P. 1981. Research to conduct an exploratory experimental and analytical investigation of alloys. AFWAL-TR-81-4046, Interim Technical Report, Contract No. F33615-75-C-1167.

2. Cadden, C. H., and Zordan, R. D. 1992. Joining of aluminides and metal matrix composites. Interim Technical Report, Contract N00140-90-C-BD42.

3. Rabinkin, A. A., Lieberman, H., Pounds, S., Taylor, T., Reidinger, F., and Siu-ching Lui. 1991. Amorphous Ti-Zr-base

Metglas® brazing filler metals. *Scripta Metallurgica* 25: 399–404.
4. Schwartz, M. M. 1987. *Brazing*, ASM International, Materials Park, Ohio, p. 435.
5. Humpston, G., and Jacobson, D. M. 1994. *Principles of Soldering and Brazing*, ASM International, Materials Park, Ohio, pp. 48–49.
6. Strychor, R., Williams, J. D., and Soffa, W. A. 1988. Phase transformations and modulated microstructures in Ti-Al-Nb alloys. *Met. Trans. A.*, pp. 225–235.
7. Marquardt, B. J., Scarr, G. K., Chesnutt, J. C., Rhodes, C. G., and Fraser, H. L. 1990. Research and development for improved toughness aluminides. Technical Report WRDC-TR-89-4133.
8. Bendersky, L. A., and Boettinger, W. J. 1993. Transformation of BCC and 82 high temperature phases to HCP and orthorhombic structures in the Ti-Al-Nb system. *Journal of Research of the National Institute of Standards and Technology* 98(5): 585–606.
9. David, S. A., Horton, J. A., Goodwin, G. M., Phillips, D. H., and Reed, R. W. 1990. Weldability and microstructure of a titanium aluminide. *Welding Journal* 69(4): 133-s to 140-s.
10. Baeslack, W. A., Mascorella, T. J., and Kelly, T. J. 1989. Weldability of a titanium aluminide. *Welding Journal* 68(12): 483-s to 498-s.
11. Cieslak, M. J., Headley, T. J., and Baeslack, W. A. 1990. Effect of thermal processing on the microstructure of Ti-26Al-11Nb: Applications to fusion welding. *Met. Trans. A.* 21A: 1273–1286.
12. Acoff, V. L., Thompson, R. G., Griffin, R. D., and Radhakrishnan, B. 1995. Effect of postweld heat treatment on Ti-14%Al-21%Nb fusion zone structure and hardness. *Welding Journal* 74(1): 1-s to 9-s.
13. Mozer, B., Bendersky, L. A., Boettinger, W. J., and Rowe, R. 1990. Neutron powder diffraction study of the orthorhombic Ti2AlNb phase. *Scripta Metallurgica* 24: 2363–2368.
14. Donachie, M. 1988. *Titanium; A Technical Guide*. ASM International, Materials Park, Ohio, pp. 28–31.
15. Massalski, T. 8. 1987. *Binary Alloy Phase Diagrams*. ASM International, Materials Park, Ohio.
16. Chesnutt, J. C., Rhodes, C. G., and Williams, J. C. 1976. Relationship between mechanical properties, microstructure and fracture topography in $\alpha + \beta$ titanium alloys. *Fractography — Microscopic Cracking Processes*. ASTM STP 600, American Society for Testing and Materials, pp. 99–138.